Developing geoacoustic seabed models for a shallow embayment with an elastic seafloor

Alec Duncan (1), Cristina Tollefsen (1), Iain Parnum (1) and Christine Erbe (1)

(1) Centre for Marine Science and Technology, Curtin University, WA, Australia

Abstract - The Western Australian Marine Science Institution (WAMSI) has carried out a multi-faceted study of Cockburn Sound, a shallow embayment south of Fremantle, prior to the establishment of a container port in the Sound. One aim of this study was to establish geoacoustic models of the seabed to facilitate numerical modelling of changes in underwater sound levels due to port construction and operation. The modelled sound levels will ultimately be used as part of an assessment of possible impacts of the new port on the marine animals that frequent the Sound. In this paper we describe the overall geology of the Sound and the process used to establish appropriate geoacoustic seabed models, which included analysis of underwater recordings of ship noise and signals from a small airgun sound source. We will also discuss techniques for modelling acoustic propagation in this environment which are complicated by the presence of high shear-speed elastic seabed layers.

1 INTRODUCTION

In 2017, the Western Australian government embarked on the Westport program, a planning initiative with the ultimate aim of moving Perth's main container port from its current location at the Fremantle inner harbour to the south-eastern shore of Cockburn Sound (see Figure 1). Cockburn Sound already has port facilities for bulk carriers and oil tankers, and hosts WA's main naval base. There is also a mix of light and heavy industry along its eastern shore. It is hardly a pristine environment, but there are significant patches of seagrass and many species of marine animals frequent the Sound, so the Western Australian Marine Science Institute (WAMSI) was commissioned to coordinate a multi-faceted study of the marine environment of the Sound to provide a baseline for environmental impact assessments for the new port.

Port construction and the increased ship traffic associated with the operation of the new port will increase underwater noise levels in Cockburn Sound, so the Centre for Marine Science and Technology's (CMST's) role has been to characterise the current underwater acoustic environment to allow this effect to be quantified and included in environmental impact assessments. This work has included making measurements of existing underwater sound levels over a twelve month period at the nine sites marked by the yellow rectangles in the right panel of Figure 1, measuring the source spectra of ships entering and leaving the northern end of the Sound over a period of two months using measurements made at the locations shown by green rectangles, and characterising acoustic propagation in various parts of the Sound using both ship noise and recordings made while a small airgun sound source was towed along the track shown by the red quadrilateral in Figure 1. The ship noise work has been described previously (Tollefsen et al. 2023), so the current paper focuses on the analysis of the airgun data, the estimation of appropriate geoacoustic parameters for the central basin and eastern (Kwinana Shelf) regions of Cockburn Sound, and the implications for predicting underwater sound levels.

2 GEOLOGICAL DESCRIPTION

As shown in the right panel of Figure 1, Cockburn Sound consists of a large central basin with an almost uniform depth of approximately 20 m, surrounded by shallow shelves of various widths and depths. The proposed location of the container port, on the eastern side of the Sound, borders the Kwinana Shelf (also known as the Eastern Shoal), which has a depth of around 10 m and will be dredged to provide access for large ships.

Skene et al. (2005) carried out an extensive study of the marine geology of Cockburn Sound which included both surficial sediment samples and vibrocores, with most of the latter being in the Central Basin and penetrating between two and three metres below the seafloor. They found that the seabed consists of a thin layer of unconsolidated sediment overlying a soft limestone known as calcarenite, which is itself variable and layered.

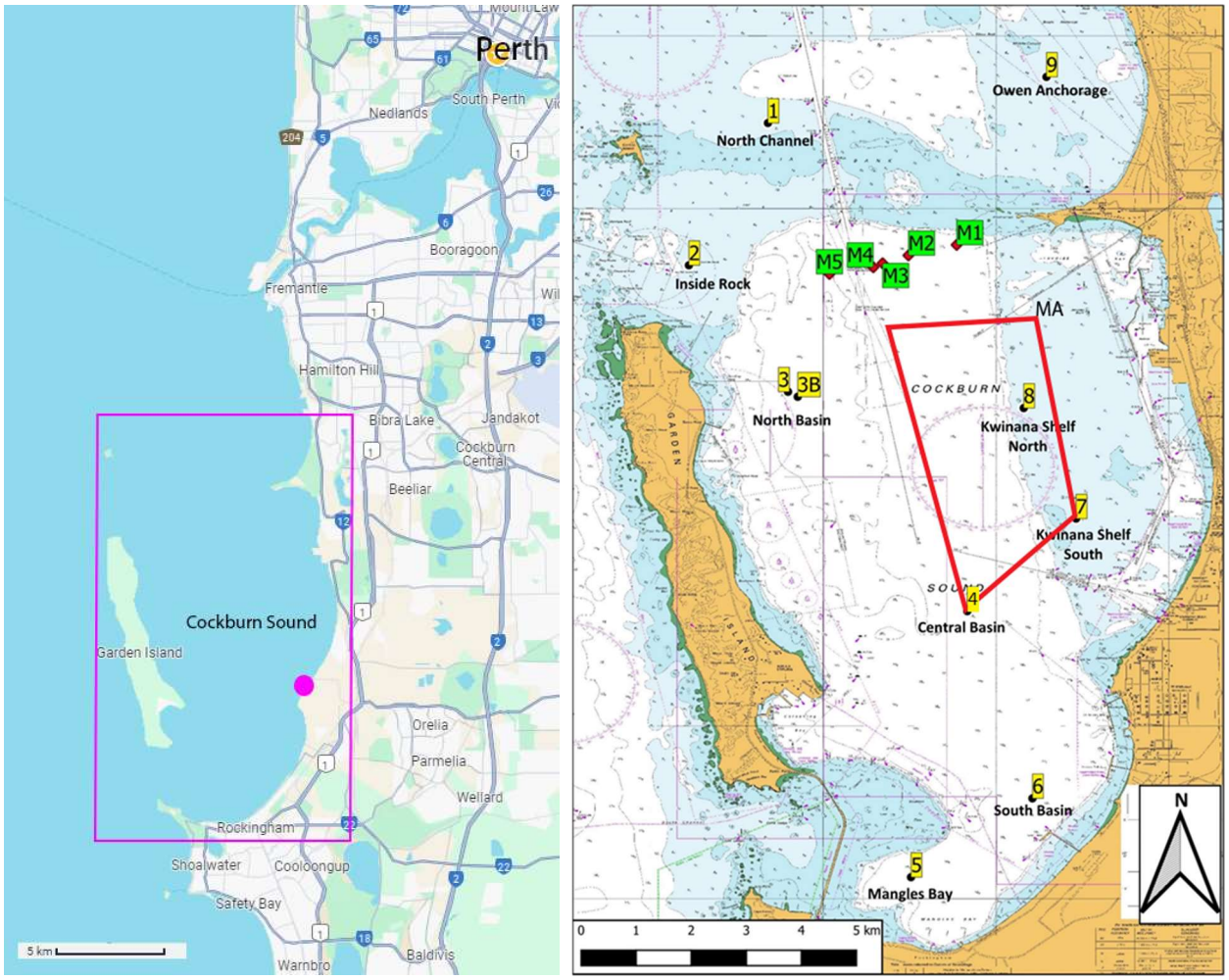

Figure 1. Left: General location diagram showing the location of Cockburn Sound (magenta rectangle) and the proposed Westport development (magenta circle). Right: detail of Cockburn Sound showing locations of ship noise measurement acoustic recordings (green rectangles), long-term acoustic recordings (yellow rectangles), and the airgun test lines (red quadrilateral). The short-term recorder deployed during the airgun measurement was at the northeast corner of the quadrilateral (MA).

A geophysical survey commissioned by Westport (Anning, 2023; Smith and Tutton, 2023) provided detailed bathymetry and sub-bottom profiler data for the Kwinana Shelf and adjacent parts of the Central Basin. These results indicated that the seabed of the Kwinana Shelf is also calcarenite, overlain with a thin veneer of unconsolidated sediment averaging about 0.5 m thick, whereas the sediment thickness can be as much as several metres in the adjacent parts of the Central Basin. In both cases the upper surface of the calcarenite is rough and the sediment fills in the hollows, leading to a relatively flat seafloor.

Calcarenite typically has a shear speed slightly less than the in-water sound speed resulting in strong coupling of the water-borne sound to shear waves in the seabed, leading to a high acoustic propagation loss at low frequencies except at a few discrete frequencies where waveguide effects dominate (Duncan et al. 2008, Duncan et al. 2013). The effect of the overlying sediment is to reduce the propagation loss, particularly at higher frequencies.

3 AIRGUN MEASUREMENTS AND HEAD WAVE ANALYSIS

Surrich Hydrographics Pty. Ltd. offered CMST the opportunity to temporarily deploy an acoustic recorder during tests of a 0.33 litre (20 cubic inch) airgun sound source in Cockburn Sound, and ran some test lines that passed close to several of CMST's long-term recorders. The temporary recorder was deployed on the seabed at location MA in Figure 1, and the vessel towing the airgun proceeded clockwise around the track shown in red. The temporary recorder was set to record continuously whereas the long-term recorders were recording for 4 minutes out of every 5 minutes.

Head wave analyses (Hall 1996) of the Site MA and Site 4 recordings were carried out for the periods when the vessel was traversing the first and third legs respectively to obtain information about the seabed characteristics in the Kwinana Shelf and Central Basin regions. Head waves (also known as lateral waves) are acoustic signals that travel via paths that include a horizontal segment along the water-seabed interface or an interface between two seabed layers (see Figure 2) and, at sufficiently long range, arrive in advance of the direct acoustic path.

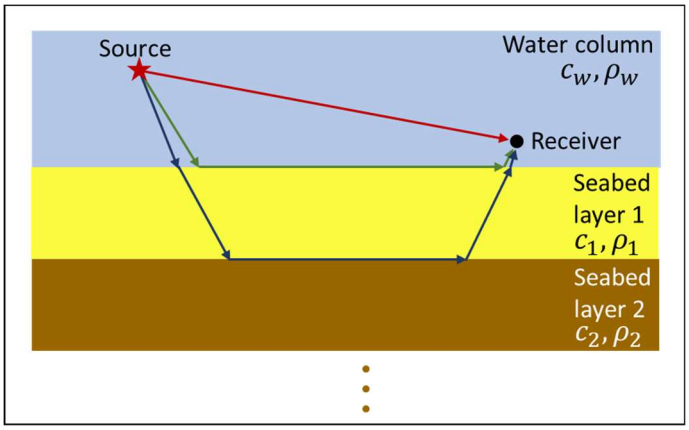

Figure 2. Diagram showing the direct acoustic path (red) and two headwave paths (green and blue) between a source and a receiver. The headwave travels along each interface at the compressional wave speed of the lower of the two media. The existence of headwaves requires that the layer sound speeds increase with increasing depth, i.e. $c_2 > c_1 > c_w$

The head wave analysis plot for the signals recorded on the temporary recorder at Site MA during the first leg (Site MA to recorder 7) is shown in Figure 3. This plot includes both low-pass (blue) and high-pass (red) filtered versions of each received signal plotted relative to the time that signal was transmitted, and offset vertically by the source to receiver range at that time. Ranges and shot times were calculated from the navigation data recorded on the boat, and zero group-delay digital filters were used for the filtering. The low-pass filtered signals emphasise the head waves, whereas the high-pass filtered signals emphasise the through-water waves. The slopes of straight lines drawn through the onset times of different waves give the corresponding sound speeds, whereas the zero-range intercepts can be used to calculate layer thicknesses (Hall 1996).

4 PROPAGATION LOSS MEASUREMENTS AND MODELLING

In order to use the data recorded during the airgun trial for propagation loss measurements it was necessary for the source waveform, and hence its spectrum, to be known. Ideally this would have been done using recordings of signals from a hydrophone located close to the airgun, however it was impractical to make recordings of this type during this particular trial. Instead, the airgun signal was simulated using CMST's airgun array model, Cagam, which is a well-tested and calibrated, physics based airgun source model (Duncan and Gavrilov, 2019). Subtracting the spectral levels of the received signal from those of the source signal yielded the propagation loss (PL).

The right-hand panels of Figure 4 and Figure 5 plot the measured narrowband (0.4 Hz resolution) PL as a function of range and frequency for airgun legs 1 (Kwinana Shelf, recorder at Site MA) and 3 (Central Basin, recorder at

location 4). The vertical white bars in the Central Basin plot are data dropouts due to the one-minute breaks that occur every four minutes in the long-term recordings

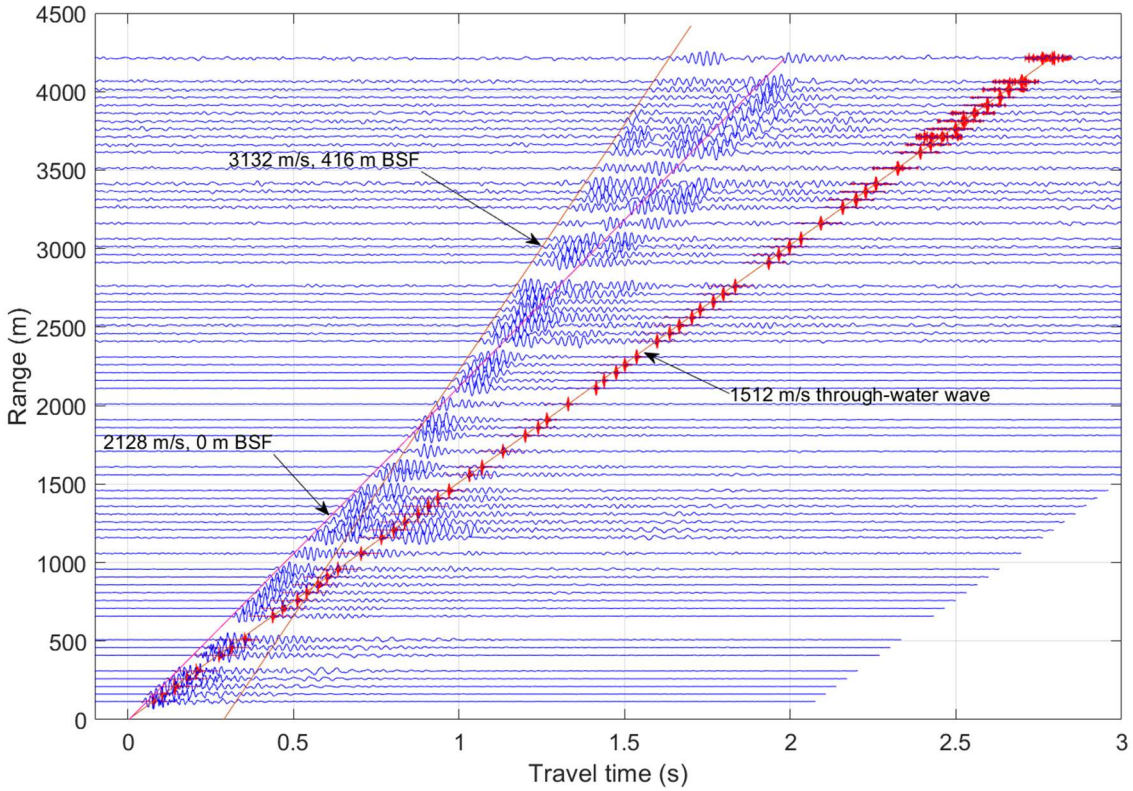

Figure 3. Stacked arrival plot for Leg 1, the track from Site MA to recorder 7, with the through-water arrival (red) and head-wave arrivals (blue) from two different seabed layers indicated. Data is from the temporary mooring at Site MA.

For both areas the propagation divides into a low-frequency regime characterised by very high propagation loss except at several discrete frequencies, and a high-frequency regime in which the propagation loss reduces with increasing frequency and an interference pattern is clearly visible. On the Kwinana Shelf the boundary between these two regimes is at about 200 Hz, whereas in the Central Basin it is at about 100 Hz. Duncan et al. (2008) and Duncan et al. (2013) show that the low-frequency, low propagation loss bands are a result of normal modes with relatively steep grazing angles corresponding to the calcarenite compressional wave critical angle, whereas the higher frequency propagation is dominated by low grazing angle normal modes. The high-frequency interference pattern is due to the presence of several modes with similar amplitudes.

The low grazing angle seabed reflectivity, and hence high-frequency propagation loss, is very sensitive to the thickness of the unconsolidated sediment layer, which was adjusted manually to obtain good qualitative agreement between measured and modelled propagation loss in the high-frequency regime. The resulting geoacoustic model parameters are listed in Table 1 and

Table 2, and the corresponding modelled propagation loss vs. range and frequency plots are shown in the left-hand panels of Figure 4 and Figure 5. Range-independent propagation loss modelling was carried out using the wavenumber integration code, SCOOTER (Porter 2018).

For both environments, the modelled and measured propagation loss plots have very similar characteristics apart from the low-frequency, low PL bands, which are much narrower and extend to higher frequencies in the model than they do in the measurements. This is a result of the model assuming a perfectly flat interface between the unconsolidated sediment and calcarenite, whereas in reality this interface has significant roughness.

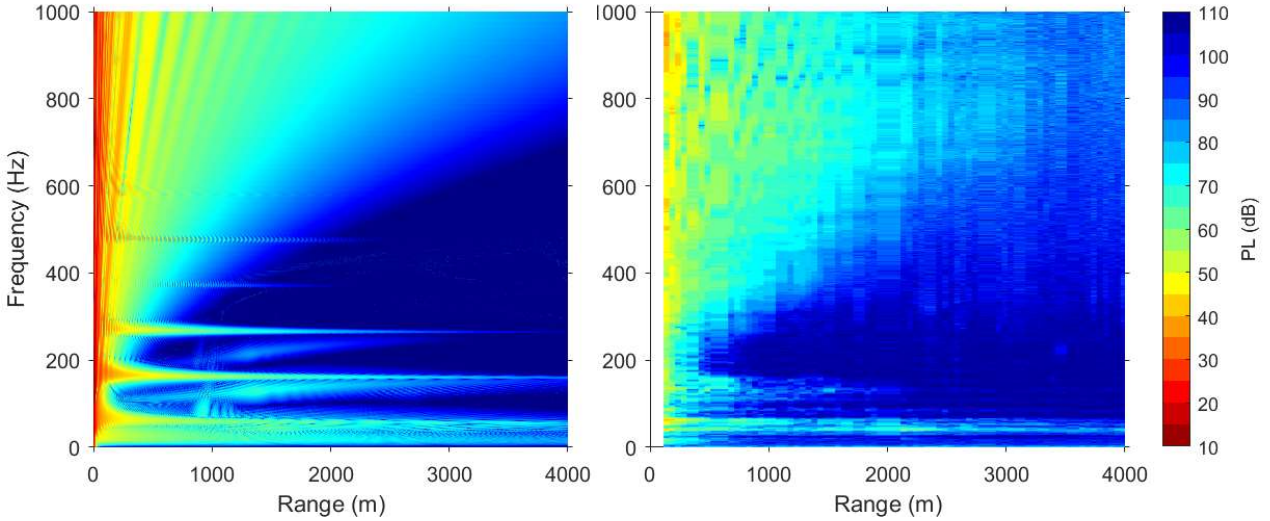

Figure 4. Modelled (left) and measured (right) propagation loss vs. range and frequency for the Kwinana Shelf, Cockburn Sound. Source depth is 3 m, water depth is 10 m and the receiver is on the seabed. The frequency resolution is 0.4 Hz.

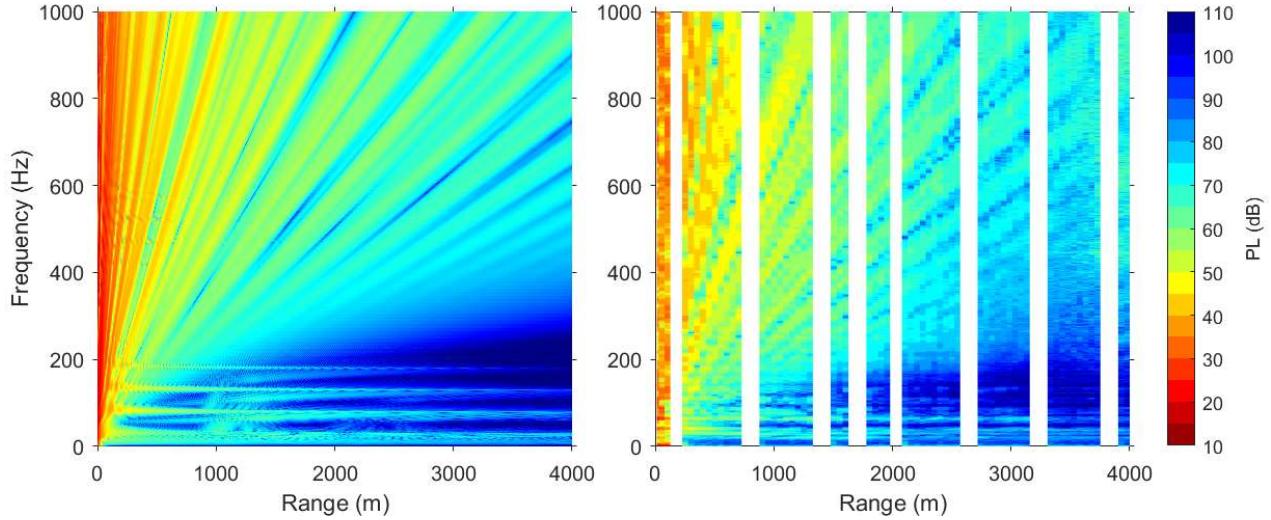

Figure 5. Modelled (left) and measured (right) propagation loss vs. range and frequency for the Central Basin of Cockburn Sound. Source depth is 3 m, water depth is 19 m and the receiver is on the seabed. The frequency resolution is 0.4 Hz.

Table 1. Geoacoustic model for the Kwinana Shelf derived from a combination of previous studies of the seabed geology of the Sound, airgun headwave analysis, and adjusting the thickness of the sandy mud layer to obtain a good match between measured and modelled propagation loss at frequencies from 500 Hz to 1 kHz. The corresponding water column sound speed is 1512 m/s.

Layer	Depth range (m below seafloor)	Density (kg/m^3)	Compressional wave speed (m/s)	Compressional wave absorption (dB/wavelength)	Shear wave speed (m/s)	Shear wave absorption (dB/wavelength)
Sandy mud	0 to 0.5 m	1694	1550	0.41	-	-
Calcarenite	0.5 to 416	2200	2128	0.1	1000	0.2
Limestone	416 to ∞	2800	3132	0.1	1500	0.2

Table 2. Geoacoustic model for the Central Basin derived from a combination of previous studies of the seabed geology of the Sound, airgun headwave analysis, and adjusting the thickness of the sandy mud layer to obtain a good match between

measured and modelled propagation loss at frequencies from 500 Hz to 1 kHz. The corresponding water column sound speed is 1512 m/s.

Layer	Depth range (m below seafloor)	Density (kg/m^3)	Compressional wave speed (m/s)	Compressional wave absorption (dB/wavelength)	Shear wave speed (m/s)	Shear wave absorption (dB/wavelength)
Sandy mud	0 to 2 m	1694	1550	0.41	-	-
Calcarenite	2 to 415	2200	2219	0.1	1100	0.2
Limestone	415 to ∞	2800	3393	0.1	1600	0.2

5 COCKBURN SOUND PROPAGATION LOSS MODELLING CHALLENGES

Underwater acoustic propagation modelling over calcarenite seabeds is a significant challenge. Calcarenite's shear speed is close to the in-water sound speed, leading to strong coupling between the in-water wave and the seabed shear wave.

Of the commonly available models that can deal with elastic seabeds, wavenumber integration models such as SCOOTER (Porter 2018) and OASES (Schmidt 2004) can accurately capture the propagation physics while remaining sufficiently computationally efficient to be useful for practical applications, but cannot deal with range dependence in the form of varying water depth, seabed properties or water column properties. As a result, even for situations that are close to range independent, such as the two examples presented in the previous section, they are unable to capture the frequency spread of the low-frequency, low propagation loss bands that occurs as a result of interface roughness.

A range dependent version of OASES exists, (Goh and Schmidt 1996, Schmidt 2004), and is available as part of the full, licensed version of the software. This is free to academic institutions for research purposes, but commercial licences are expensive. Its suitability for modelling acoustic propagation in this environment is yet to be evaluated.

Complex normal mode codes such as ORCA (Westwood et al. 1996) have been successfully used to model range independent propagation over calcarenite seabeds (Hall 2004), and several attempts have been made to extend this approach to problems with weak range-dependence using the adiabatic normal mode method (Hall 2004, Koessler 2016). However these are research level codes and are not readily available.

The authors have attempted to use the elastic parabolic equation code, RAMS (Collins 1993b) for this environment but have been unable to achieve numerically stable solutions. More advanced parabolic equation codes (e.g. Collis 2008) have better stability and have been successfully applied to similar problems (Duncan et al. 2013) but remain research level codes that are difficult to obtain and use.

In the high-frequency regime where the propagation is dominated by low grazing angle modes it is possible to get around these problems by replacing the elastic calcarenite with an "equivalent" fluid with parameters chosen to give as close as possible a match between the plane-wave reflection coefficients of water/calcarenite and water/equivalent fluid interfaces at low grazing angles. The calcarenite can then be replaced by the equivalent fluid in the seabed geoacoustic model, which can then be used as input to a fluid propagation model. The equivalent fluids typically have very high attenuation, so any deeper elastic layers can be ignored.

This approach is illustrated for the Kwinana Shelf environment in Figure 6 and Figure 7. In this example the fluid parabolic equation code RAMGeo (Collins 1993a) was used to calculate the propagation loss using the fitted equivalent fluid geoacoustic model. The fit was carried out by keeping the density of the fluid the same as that of the calcarenite and then doing a brute-force 2D search for the sound speed and attenuation that minimised the sum of the squared differences between the magnitudes of the planewave reflection coefficients over the grazing

angle range 0° to 30°. The plane wave reflection coefficient curves were calculated using equations from Section 1.6 of Jensen et al. (2011). The resulting geoacoustic model is given in Table 3 for the Kwinana Shelf and in Table 4 for the Central Basin

As can be seen in Figure 7, this approach leads to excellent agreement between the high-frequency interference patterns produced by SCOOTER and RAMGeo but, as expected, the RAMGeo result does not include the horizontal, low propagation loss bands seen in the SCOOTER result. This is because the low loss bands are a result of propagating modes with grazing angles corresponding to the peak in the calcarenite reflection coefficient curve seen at 42° in Figure 6, which are not captured by the equivalent fluid model. From Figure 4 it is apparent that seabed roughness effects are likely to remove these bands at frequencies above 200 Hz, so the equivalent fluid / RAMGeo result would be expected to be the more accurate of the two for frequencies above 200 Hz. However, in the low-frequency regime below 200 Hz, the RAMGeo result grossly overestimates the propagation loss.

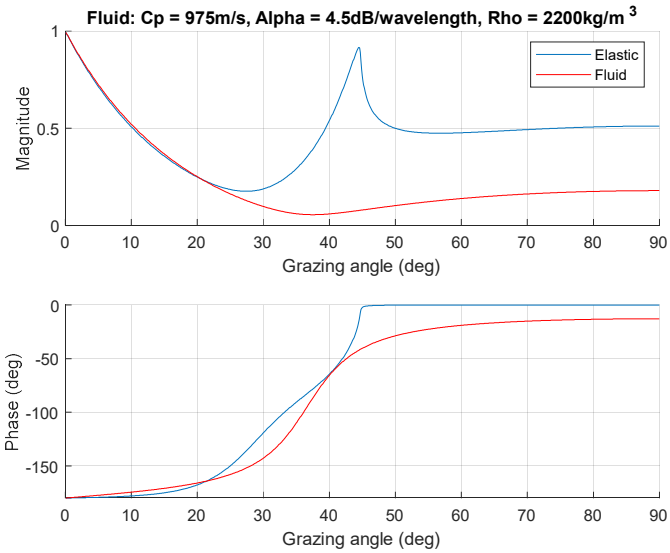

Figure 6. Plane-wave reflection coefficient magnitude and phase as a function of grazing angle for a water-calcarenite interface (Kwinana Shelf parameters) (blue) and with the calcarenite replaced by an equivalent fluid with the properties given in the title (red).

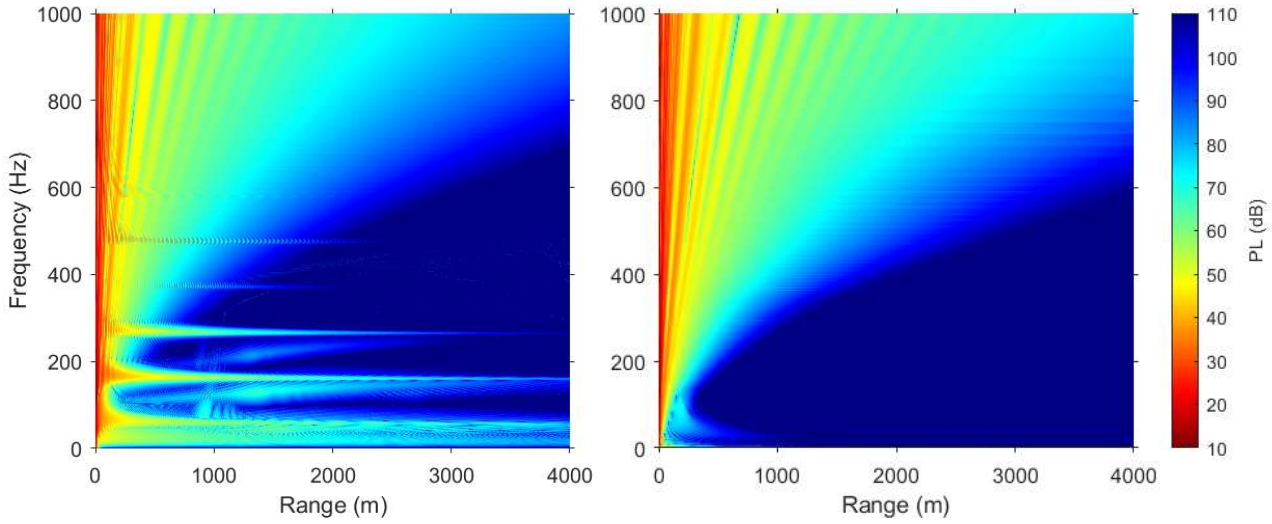

Figure 7. Propagation loss vs. range and frequency for the Kwinana Shelf calculated using SCOOTER with the full geoacoustic model (left) and calculated using RAMGeo with an equivalent fluid geoacoustic model (right).

Table 3. Equivalent fluid geoacoustic model for the Kwinana Shelf suitable for range dependent propagation modelling at frequencies of 200 Hz and above.

Layer	Depth range (m below seafloor)	Density (kg/m^3)	Compressional wave speed (m/s)	Compressional wave absorption (dB/wavelength)
Sandy mud	0 to 0.5 m	1694	1550	0.41
Calcarenite	0.5 to ∞	2200	975	4.5

Table 4. Equivalent fluid geoacoustic model for the Central Basin suitable for range dependent propagation modelling at frequencies of 200 Hz and above.

Layer	Depth range (m below seafloor)	Density (kg/m^3)	Compressional wave speed (m/s)	Compressional wave absorption (dB/wavelength)
Sandy mud	0 to 2 m	1694	1550	0.41
Calcarenite	2 to ∞	2200	1096	0.7

6 CONCLUSIONS AND FURTHER WORK

A considerable body of pre-existing knowledge about the seabed geology of Cockburn Sound, together with recordings of signals from a small airgun, made it possible to derive geoacoustic models for the Kwinana Shelf and Central Basin that gave very good agreement between measured and modelled propagation loss within the limitations of the available propagation modelling codes. It may be possible to improve on these results using numerical geoacoustic inversion methods, however this was not considered worthwhile given the limitations of the propagation codes when applied to this environment.

Good results were obtained at frequencies above 200 Hz using the parabolic equation code RAMGeo with an equivalent fluid seabed model, and this can be readily extended to deal with range-dependent environments. However, this approach would give misleading results at lower frequencies and range dependent modelling at frequencies below 200 Hz remains an unsolved problem.

Further work will investigate the suitability of the range dependent version of OASES for this task, although the high cost of a commercial licence for this software is likely to make this an unattractive approach for environmental impact assessments. A practical work-around may be to use empirical transmission loss vs range fits to the measured data, with the proviso that they are only valid for the same source and receiver depths as the measurements, and for environments similar to those in which the measurements were made.

We would also like to extend this work to ground-truthing modelling of range-dependent propagation between a source in the Central Basin and a receiver on the Kwinana Shelf and vice-versa.

ACKNOWLEDGEMENTS

This work was funded by the Western Australian Marine Science Institution's WAMSI Westport Marine Science Program.

The authors would like to thank Justin Anning from Surrich Hydrographic Pty. Ltd. for the opportunity to make the recordings of the airgun signals and for providing the associated metadata that made it possible to carry out the analysis described in this paper.

REFERENCES

Anning, J, (2023) "DOT415821 "Westport Marine Geophysical Survey Area1 Factual Report", *Surrich Hydrographics report on project SH20221201*, August 2023.

Collins MD (1993a) “A split-step Pade solution for the parabolic equation method”. *J. Acous. Soc. Am., 93*(4), 1736-1742.

Collins MD (1993b) “An energy-conserving parabolic equation for elastic media” *J. Acous. Soc. Am., 94*(2), 975-982.

Collis JM, Siegmann WL, Jensen FB, Zampolli M, Kusel ET, Collins MD (2008) “Parabolic equation solution of seismo-acoustics problems involving variations in bathymetry and sediment thickness” *J. Acous. Soc. Am.,123 (1), 51-55.*

Duncan AJ, Gavrilov A and Hu T (2008), “Using offshore seismic surveys as acoustic sources of opportunity for geoacoustic inversion”, *Proceedings, Acoustics '08*, Paris, June 29 to July 08.

Duncan AJ, Gavrilov AN, McCauley, RD, Parnum IM, Collis JM (2013) “Characteristics of sound propagation in shallow water over an elastic seabed with a thin cap-rock layer”, *J. Acous. Soc. Am*. 134 (1), pp. 207-215.

Duncan AJ, Gavrilov AN (2019) "The CMST Airgun Array Model—A Simple Approach to Modeling the Underwater Sound Output From Seismic Airgun Arrays", *IEEE J. Oc. Eng.*, 44 (3), pp 589-597, DOI: 10.1109/JOE.2019.2899134, July 2019.

Goh JT, Schmidt H (1996) “A hybrid coupled wave-number integration approach to range-dependent seismoacoustic modelling” *J. Acoust. Soc. Am.*, 100 (3) pp 1409-1420.

Hall MV (1996) "Measurement of seabed sound speeds from Head waves in shallow water", *IEEE J. Oc. Eng*., 21 (4), pp.413-422.

Hall MV (2004) "Preliminary Analysis of the Applicability of Adiabatic Modes to Inverting Synthetic Acoustic Data in Shallow Water over a Sloping Sea Floor." *IEEE J. Oc. Eng.*, 29 (1): 51-58.

Jensen FB, Kuperman WA, Porter, MB, Schmidt H (2011) *Computational Ocean Acoustics*, 2nd Ed. Springer, ISBN 978-1-4419-8677-1.

Koessler MW (2016) *Modelling of Underwater Acoustic Propagation over Elastic, Range-Dependent Seabeds*, PhD thesis, Curtin University, Australia.

Porter MB (2018) “Acoustics Toolbox” https://oalib-acoustics.org/AcousticsToolbox/index_at.html.

Schmidt H (2004) “OASES - Ocean Acoustics and Seismic Exploration Synthesis”, https://acoustics.mit.edu/faculty/henrik/oases.html.

Skene D, Ryan D, Brooke B, Radke L (2005) “Report on geomorphology and sediments of Cockburn Sound.” Coastal CRC *Coastal Water Habitat Mapping Project, Milestone Report CG4.04A*.

Smith JV and Tutton M (2023), “DOT415821 Westport Geophysical Survey Interpretative Report, R4”, *Surrich Hydrographics report MEL2023-0118A*.

Tollefsen C, Duncan AJ, Parnum I (2023) “Propagation of ship noise in shallow water over a high shear-speed seabed”, Paper presented at Acoustics 2023, joint conference of the Acoustical Society of America and the Australian Acoustical Society, Sydney, Australia, 18 to 22 November.

Westwood EK., Tindle CT, Chapman NR (1996) "A Normal Mode Model for Acousto-Elastic Ocean Environments." *J. Acous. Soc. Am*. 100 (6): 3631-3645.